EUROPHYSICS LETTERS 15 February 2003

Europhys. Lett., **61** (4), pp. 492–498 (2003)

Wall effects on granular heap stability

S. Courrech du Pont[1], P. Gondret[1], B. Perrin[2] and M. Rabaud[1]

[1] *FAST Universités Paris 6 & 11 et CNRS (UMR 7608)*
Bât. 502, campus universitaire, 91405 Orsay cedex, France
[2] *LPMC Universités Paris 6 & 7, ENS et CNRS (UMR 8551)*
24 rue Lhomond, 75005 Paris, France

(received 29 July 2002; accepted in final form 6 December 2002)

PACS. 45.70.Ht – Avalanches.
PACS. 45.70.-n – Granular systems.
PACS. 45.05.+x – General theory of classical mechanics of discrete systems.

Abstract. – We investigate the effects of lateral walls on the angle of movement and on the angle of repose of a granular pile. Our experimental results for beads immersed in water are similar to previous results obtained in air and to recent numerical simulations. All of these results, showing an increase of pile angles with a decreasing gap width, are explained by a model based on the redirection of stresses through the granular media. Two regimes are observed depending on the bead diameter. For large beads, the range of wall effects corresponds to a constant number of beads, whereas it corresponds to a constant characteristic length for small beads as they aggregate via van der Waals forces.

A characteristic of a sand pile is that it forms a non-zero angle to the horizontal. Two angles can be defined for a heap of granular matter: the angle of repose θ_{r}, under which no flow can occur, and, a few degrees larger, the maximum angle of stability θ_{m} first noticed by Bagnold [1]. This angle, also called the angle of movement, is the one at which an avalanche spontaneously occurs at the surface of the pile, making the slope angle relax to the angle of repose. Between these two angles is a region of bistability as the heap can be static ("solid state") or flowing ("liquid state"). The values of these two angles have been known for long to depend on many parameters, namely the shape, the roughness, the size distribution and the packing fraction of grains, as well as the packing history [2]. Humidity, by introducing cohesion through capillary bridges between grains, is known to strongly increase the stability of a heap [3]. The presence of close lateral walls, by changing the boundary conditions, also increases the stability of a heap, as both angles θ_{m} and θ_{r} increase when the gap width between the confining walls decreases [4]. This is often explained qualitatively by the presence of particle arches between the walls [5–7]. Particle arches or divergence of force networks lead to many remarkable effects. The saturation of the pressure at the bottom of containers, known as the Janssen effect [8], makes hourglasses flow at constant speed. In silos, arch formation may lead to a complete jamming of the flow, with potential damages for industry. Most of laboratory model experiments on granular physics are led using experimental set-up where the granular medium is confined. Lateral wall effects on pile angles have recently been studied both experimentally [5–7] and numerically [7]. Grasselli and Herrmann [5] measured the angle of repose for dry glass beads of different diameter d ($0.1 \leq d \leq 0.5\,\mathrm{mm}$), by slowly filling from one side a rectangular glass cell of gap width b in the range $1 < b < 10\,\mathrm{mm}$.

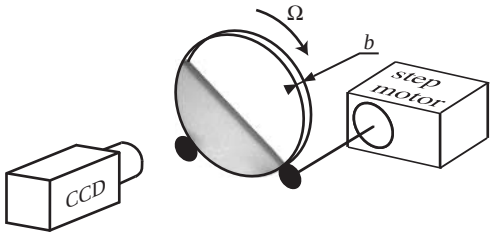

Fig. 1

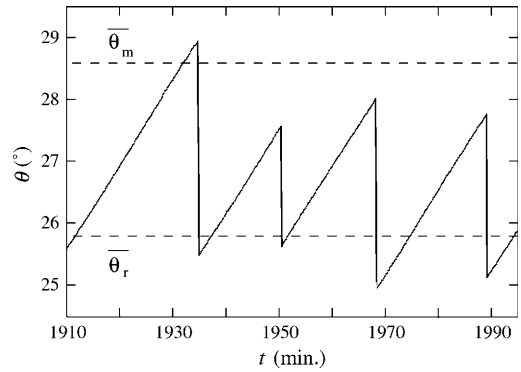

Fig. 2

Fig. 1 – Sketch of the rotating drum experiment.

Fig. 2 – Time evolution of the slope angle θ for glass beads of diameter $d = 1.85\,\mathrm{mm}$ totally immersed in water, in a cylinder of gap width $b = 15.5\,\mathrm{mm}$ rotating at the angular velocity $\Omega = 4 \cdot 10^{-3}\,\mathrm{rpm}$. From the whole experiment, $\overline{\theta_\mathrm{m}} = 28.6 \pm 0.8^\circ$ and $\overline{\theta_\mathrm{r}} = 25.8 \pm 0.5^\circ$ (dashed lines).

Boltenhagen [6] measured the angle of movement of dry millimetric glass beads ($1 \leq d \leq 4\,\mathrm{mm}$) by tilting a Plexiglas rectangular cell ($8 < b/d < 100$). More recently, Zhou and co-workers [7] have investigated the angle of repose both experimentally and numerically by discharging a rectangular box ($4 < b/d < 24$) filled with dry monodisperse glass spheres ($1 \leq d \leq 10\,\mathrm{mm}$). In all these experiments the wall effects are only controlled by the smallest dimension (gap width b), *i.e.* other cell dimensions do not play any role. All these authors [5–7] observed that the pile angles θ_r and θ_m decrease with an increasing gap width towards constant values, and fitted their results by the empirical exponential law

$$\theta = \theta_\infty[1 + \alpha \exp[-b/b^*]], \tag{1}$$

with three fitting parameters: θ_∞ is the angle value when b tends towards infinity, b^* is the characteristic length scale of wall effect and α is a parameter of order 1 [5–7]. This description leads one to wonder which parameters govern the characteristic length scale b^* of wall effects. Boltenhagen found for millimetric beads that the characteristic number of beads n^*, defined as $n^* = b^*/d$, decreases slightly with increasing bead diameters [6]. The results of Zhou *et al.* [7] can be interpreted as a constant n^* value (~ 6), independent of the particle size. On the contrary, Grasselli and Herrmann found for submillimetric beads that n^* strongly increases as the bead diameter decreases, leading to a constant value of b^* ($\sim 9\,\mathrm{mm}$), and evoked the cohesion due to humidity as a possible explanation for this unexpected behaviour [5].

We have experimentally studied for a large range of bead diameters the lateral wall effects on both the angle of movement and the angle of repose of a packing of glass spheres. To eliminate the effect of possible capillary bridges between beads and to reduce the electrostatic forces, glass beads are totally immersed in water. We also propose a physical modelling of the wall influence on pile angles that is based on the Janssen effect [8], *i.e.* on the pressure saturation that occurs with depth in confined granular media.

A sketch of our experimental set-up is displayed in fig. 1. It consists of a rotating cylinder of inner diameter $D = 17\,\mathrm{cm}$, half-filled with rather monodisperse sieved glass beads of mean diameter d (with a dispersion of 10%). The granular pile is totally immersed in water and confined between two parallel glass or Plexiglas endwalls separated by a gap whose width b can be

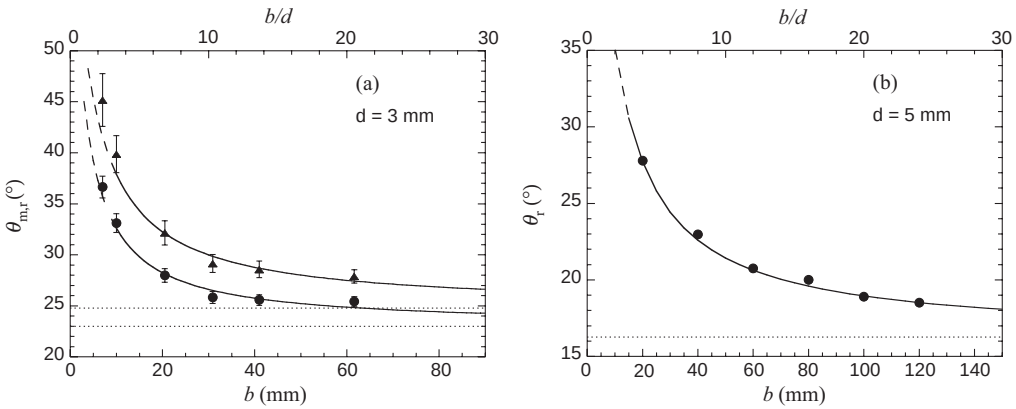

Fig. 3 – Pile angles $\theta_{\mathrm{m,r}}$ as a function of the gap width b. (a) Our experimental data for θ_{m} (▲) and θ_{r} (●) for $d = 3\,\mathrm{mm}$ glass beads in water (error bars correspond to the standard deviation). (b) Numerical results of [7] for $d = 5\,\mathrm{mm}$ glass beads in vacuum. Solid lines correspond to our model equation (6) with (a) ($\theta_{\mathrm{m}}^{\infty} = 24.75°$, $B_{\mathrm{m}} = 6\,\mathrm{mm}$) and ($\theta_{\mathrm{r}}^{\infty} = 23°$, $B_{\mathrm{r}} = 4\,\mathrm{mm}$) and (b) ($\theta_{\mathrm{r}}^{\infty} = 16.25°$, $B_{\mathrm{r}} = 9.8\,\mathrm{mm}$). Horizontal dotted lines correspond to the asymptotic values $\theta_{\mathrm{r}}^{\infty}$ and $\theta_{\mathrm{m}}^{\infty}$.

varied thanks to rubber wedges. The cylinder lies on two horizontal parallel axes, one of which is driven by a micro-step motor followed by a reducer, so that the cylinder smoothly turns at a constant angular velocity Ω. The angular velocity Ω is chosen low enough to be in the intermittent regime of avalanches [9], so that the typical time between two avalanches is much larger than the typical avalanche duration. With a CCD video camera set in the laboratory frame and aligned with the cylinder axis, images are taken at regular time intervals, then analysed in order to track the pile interface. This interface is found to be plane, thus well characterised by its mean slope angle θ. Any change of $0.01°$ for the mean slope angle can be detected.

A typical time evolution of the mean slope angle $\theta(t)$ is displayed in fig. 2. The slope angle increases linearly with time at the rate Ω, as the pile is in solid rotation with the drum, up to the maximum angle of stability θ_{m}. Then it quickly relaxes through a surface avalanche down to the angle of repose θ_{r}. Over all the duration of one experiment (more than one hundred events), we calculate the mean values $\overline{\theta_{\mathrm{m}}}$ and $\overline{\theta_{\mathrm{r}}}$. Henceforth, we focus on these mean values, and relieve the mean bar notations. Note that the fluctuations around these mean values are found to be smaller for the angle of repose than for the angle of movement. In the present experiments we have made the diameter of the glass beads vary in the range $0.1\,\mathrm{mm} < d \leq 3\,\mathrm{mm}$, and the gap width of the cylinder in the range $1 \leq b \leq 60\,\mathrm{mm}$ and $2 < b/d < 100$. The cylinder aspect ratio b/D remains small ($6 \cdot 10^{-3} \lesssim b/D \lesssim 3 \cdot 10^{-1}$) in order to avoid any diameter effects. This explains that observed avalanches concern the whole width of the pile and leave the interface flat, contrary to large b/D studies [10].

Figure 3a shows typical variations of both the angle of movement θ_{m} and the angle of repose θ_{r} as a function of the gap width b. Increasing the gap makes θ_{m} and θ_{r} decrease towards respective constant values $\theta_{\mathrm{m}}^{\infty}$ and $\theta_{\mathrm{r}}^{\infty}$. One can also notice that the avalanche amplitude $(\theta_{\mathrm{m}} - \theta_{\mathrm{r}})$ increases with a decreasing gap width, as has been previously reported [11]. We propose now a simple physical model taking into account the lateral wall effects on pile angles. The presence of confining walls is well known to play a key role for the saturation of the normal stresses with the depth of a granular pile. Let us first look at this Janssen effect in our configuration. In a pile making an angle θ to the horizontal, let us consider a thin layer of thickness $\mathrm{d}h$, length $\mathrm{d}l$ and width b (corresponding to the whole gap) located at the depth h

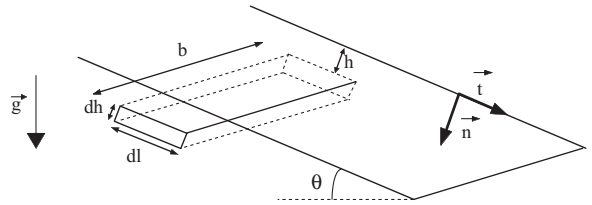

Fig. 4 – Scheme of the pile described as a continuous medium.

under the pile surface (fig. 4). At equilibrium, the $\vec{n}$ component (normal to the pile interface) of the weight of the layer is balanced by the gradient of the stress σ_{nn} (here called the pressure p) and by friction on the walls. Following the Janssen analysis, a part of the pressure (that is supposed to depend only on h) is redistributed normal to each wall through the Janssen coefficient K which induces a fully mobilised friction force with a friction coefficient μ so that the equilibrium equation along the $\vec{n}$-direction writes

$$\rho g \cos\theta b \,\mathrm{d}h \,\mathrm{d}l + [p(h) - p(h + \mathrm{d}h)]b \,\mathrm{d}l - 2K\mu p(h) \,\mathrm{d}h \,\mathrm{d}l = 0, \tag{2}$$

where ρ is the mean pile density and g is the gravity acceleration. By integrating eq. (2) we obtain the pressure expression

$$p(h) = \rho g \cos\theta \frac{b}{2K\mu}\left[1 - \exp\left[-\frac{2K\mu h}{b}\right]\right]. \tag{3}$$

A surface avalanche starts when the equilibrium along the $\vec{t}$-direction (tangent to the pile interface) is broken for a layer of depth h_{crack}. Without lateral walls, this arises when the pile reaches the critical angle $\theta_{\mathrm{m}}^{\infty}$ to the horizontal, *i.e.* when the $\vec{t}$ component of the layer weight reaches the critical value

$$F^{\infty} = \rho g b h_{\mathrm{crack}} \,\mathrm{d}l \sin\theta_{\mathrm{m}}^{\infty}. \tag{4}$$

When lateral walls are present, the heap stability increases because of the friction force on the walls along the $\vec{t}$-direction. Thus, when the lateral walls are b apart, we assume that the avalanche starts at the same h_{crack} for a larger critical pile angle $\theta_{\mathrm{m}}(b)$ given by

$$\rho g b h_{\mathrm{crack}} \,\mathrm{d}l \sin\theta_{\mathrm{m}}(b) = F^{\infty} + 2K\mu \,\mathrm{d}l \int_0^{h_{\mathrm{crack}}} p(h) \,\mathrm{d}h. \tag{5}$$

By introducing the pressure expression (eq. (3)) and the F^{∞} expression (eq. (4)) in eq. (5) we obtain the following equation that relates the movement angle θ_{m} to the gap width b:

$$\frac{\sin\theta_{\mathrm{m}}(b) - \sin\theta_{\mathrm{m}}^{\infty}}{\cos\theta_{\mathrm{m}}(b)} = 1 - \frac{b}{B_{\mathrm{m}}}\left[1 - \exp\left[-\frac{B_{\mathrm{m}}}{b}\right]\right], \tag{6}$$

which reduces for $b \gg B_{\mathrm{m}}$ to

$$\frac{\sin\theta_{\mathrm{m}}(b) - \sin\theta_{\mathrm{m}}^{\infty}}{\cos\theta_{\mathrm{m}}(b)} \simeq \frac{B_{\mathrm{m}}}{2b}, \tag{7}$$

where B_{m} is the characteristic length of lateral wall effects given by

$$B_{\mathrm{m}} = 2K\mu h_{\mathrm{crack}}. \tag{8}$$

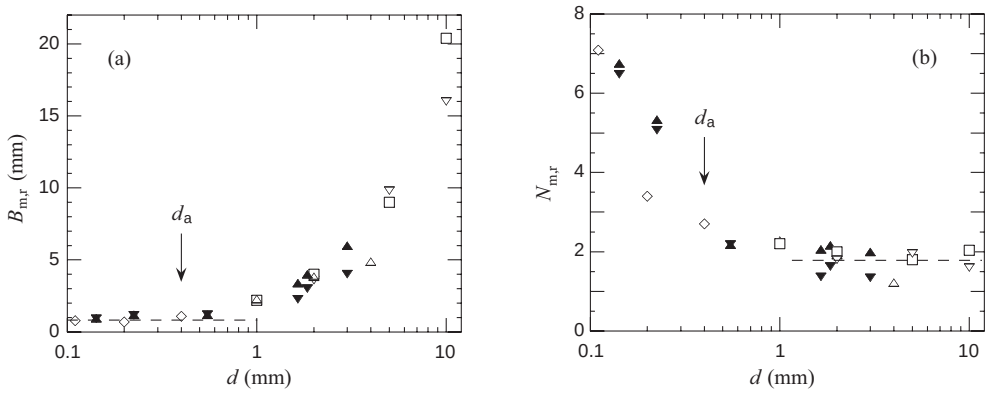

Fig. 5 – Characteristic range of wall effects $B_{m,r}$ (a) and $N_{m,r} = B_{m,r}/d$ (b) as a function of the bead diameter d extracted from our experimental data for θ_m (▲) and θ_r (▼) in water and from experimental data of ref. [5] for θ_r in air (◇), ref. [6] for θ_m in air (△), and ref. [7] for θ_r in air (□), and from the numerical data of ref. [7] for θ_r in vacuum (▽).

Equation (6) involves the two physical parameters θ_m^∞ and B_m. It predicts that θ_m decreases when b increases and reaches θ_m^∞ when b tends towards infinity. For the typical value $\theta_m^\infty = 25°$, the maximal value θ_m^0 that would be obtained for $b = 0$ is equal to 62°. It is worth noting that the θ_m decrease does not follow a classical exponential decay (here $(\theta_m(b) - \theta_m^\infty)/(\theta_m^0 - \theta_m^\infty) = 1/e$ for $b \approx 2B_m$). Indeed, θ_m tends more slowly towards its asymptotic value θ_m^∞. In the Janssen analysis, the granular medium is considered as a continuum. Already questionable considering a static pile, this hypothesis is all the more questionable considering a flowing layer. Nevertheless, the Janssen model enables one to account for dynamic effects, such as the constant flow of hourglasses. Assuming that eq. (6) can also be applied just before an avalanche stops, one obtains the same expression for the angle of repose $\theta_r(b)$ whose asymptotic value is θ_r^∞ and characteristic length is $B_r = 2K\mu h_{freeze}$, h_{freeze} being the flowing layer height when the flow is about to stop. Note that both K and μ coefficients could be slightly different in B_m and B_r expressions as they correspond either to a static or a dynamic case.

In fig. 3 the two typical data sets from our experiments (a) and from the numerical simulations of Zhou *et al.* [7] are fitted with our model equation (6). These curves illustrate the good agreement we obtain between our model and all the data sets. The exponential decay used in refs. [5–7] fits all the data as well but it involves three fitting parameters, and is not based on any physical argument. Note that our continuum model is only pertinent for $b/d \gtrsim 3$ (suggested by the dashed lines in fig. 3) as the stress redistribution needs a few beads to be effective. In this range, eq. (7) is a very good approximation of the full equation (6).

In order to extract the evolution of the characteristic lengths $B_{m,r}$ with the bead diameter d, our experimental data but also data from the three former studies mentioned above [5–7] have been analysed in the light of this model. For our experiments the asymptotic angle values are all found between 22.5° and 25.5° for θ_m^∞ and between 22° and 24.5° for θ_r^∞. Figures 5a and b show the characteristic length $B_{m,r}$ and the corresponding characteristic number of beads $N_{m,r} = B_{m,r}/d$ as a function of the bead diameter d for our experiments in water and other results in air [5–7]. Considering this, all data collapse remarkably well onto a single curve. This suggests that neither the Janssen coefficient K nor the friction coefficient μ for glass beads in air or in water, with glass or Plexiglas lateral walls, change much from one experimental set-up to another [12]. However, according to the different ways of making

a heap (in water or in air, with a rotating drum or by the discharging method, etc.), the asymptotic values $\theta^{\infty}_{\mathrm{m,r}}$ vary (*e.g.*, they vary from 14° to 26°).

Figures 5a and b clearly show two regimes depending on the bead diameter. For large beads ($d > 1\,\mathrm{mm}$), $N_{\mathrm{m,r}}$ is found constant ($N_{\mathrm{m,r}} \approx 1.8 \pm 0.4$), leading to a characteristic length $B_{\mathrm{m,r}}$ proportional to d. For small beads ($d < 1\,\mathrm{mm}$), $N_{\mathrm{m,r}}$ strongly increases with decreasing bead diameters, leading to a constant characteristic length ($B_{\mathrm{m,r}} \approx 0.8 \pm 0.2\,\mathrm{mm}$) as was previously observed in air [5].

Let us first focus on large beads. In that case the relevant parameter that governs wall effects on pile angles is then the number $N_{\mathrm{m,r}}$ of beads in the gap width, as $N_{\mathrm{m,r}}$ is constant. Since $N_{\mathrm{m,r}}$ is of the order of two beads (cf. fig. 5b), 63% of wall effects on pile angles have disappeared for a gap width $b \approx 4d$. This constant number of beads, which can be interpreted as the consistent length of a force network, can be understood seeing the stress redistribution to the lateral walls acting geometrically through contact networks. One may notice that such a characteristic length, of the order of a few bead diameters, results from different experiments [13]. Moreover, regarding eq. (8) and considering the typical value $K\mu \sim 0.2$ [8], h_{crack} and h_{freeze} are found roughly equal to 4-5 bead diameters, which is consistent with the thickness of the granular flowing layer we observed.

If we consider our results, N_{r} is slightly smaller than N_{m}. Apart from the fact that h_{crack} and h_{freeze} can possibly be different, this difference may be explained by a lower value of the friction coefficient μ and/or of the Janssen coefficient K in the dynamical case [14].

Let us look now at the small-bead regime (typically $d < 1\,\mathrm{mm}$). For small beads the characteristic range of wall effects $B_{\mathrm{m,r}}$ is no longer proportional to d but tends, for vanishing bead diameters, to a constant value equal to roughly 0.8 mm, regarding experiments performed both in air and in water (fig. 5a). One possible explanation for this phenomenon is that sub-millimetric beads aggregate. Cohesion due to capillary bridges between grains has been evoked as a possible explanation for aggregate formation in air [5]. However, capillary bridges cannot form in our fully immersed packing. Moreover, the accordance between our experiments in water and experiments in air suggests to look for a unique cause that explains aggregates. We show here that surface forces such as van der Waals forces between beads lead to aggregates and can explain the constant value of $B_{\mathrm{m,r}}$.

The van der Waals energy between two spheres of respective radius R_1 and R_2, a distance δ apart is $W(\delta) = -AR_1R_2/6\delta(R_1 + R_2)$, where A is the Hamaker constant [15]. We can estimate the aggregate size so that a bead belongs to the aggregate if the resulting van der Waals forces are larger than the whole aggregate weight. Our glass beads (commercial crushing glass beads) are rough with a roughness size that is independent of the bead size and that is of the order of one micron. Then, van der Waals forces between two beads of radius R_1 in contact may be calculated between a bead and a roughness of radius R_2 ($R_2 \ll R_1$) at a distance of perfect contact, *i.e.* corresponding to the molecular size δ [16]. Considering three contacts for a peripheral bead with the rest of the aggregate, the aggregate diameter is

$$d_{\mathrm{a}} = \left(\frac{3AR_2}{\pi c_0 \delta^2 \Delta\rho g} \right)^{1/3}, \tag{9}$$

where c_0 is the packing fraction and $\Delta\rho$ the apparent bead density. The aggregate diameter, thus found independent of the particle size, is $d_{\mathrm{a}} \approx 0.3\,\mathrm{mm}$ for glass beads immersed in water and $d_{\mathrm{a}} \approx 0.5\,\mathrm{mm}$ for glass beads in dry air (with $A = 10^{-20}\,\mathrm{J}$ and $\Delta\rho = 1500\,\mathrm{kg\,m^{-3}}$ in the water case, $A = 10^{-19}\,\mathrm{J}$ and $\Delta\rho = 2500\,\mathrm{kg\,m^{-3}}$ in the dry air case, $\delta = 0.2\,\mathrm{nm}$, $R_2 = 1\,\mu\mathrm{m}$, $c_0 = 0.6$ and $g = 9.8\,\mathrm{m\,s^{-2}}$). One observes in fig. 5 that the value $d_{\mathrm{a}} \approx 0.4\,\mathrm{mm}$ predicts well the transition between the two regimes. Furthermore, as well as $B_{\mathrm{m,r}} \approx 2d$ for large beads ($d > d_{\mathrm{a}}$) $B_{\mathrm{m,r}} \approx 2d_{\mathrm{a}} \approx 0.8\,\mathrm{mm}$ for small beads ($d < d_{\mathrm{a}}$).

Thus, the characteristic length of wall effects $B_{\mathrm{m,r}}$ always corresponds to a constant number of either beads (for $d > d_{\mathrm{a}}$) or aggregates (for $d < d_{\mathrm{a}}$).

The presence of close lateral walls increases the heap stability in the same way in air and in water. This phenomenon can be explained by particle arches that direct a part of the weight to the walls, thus inducing friction. Our physical model based on arching effects is in accordance with our experimental results and with those of former studies. For non-cohesive spheres the characteristic length of wall effects on pile angles is found to be proportional to the bead diameter d. By contrast, due to van der Waals forces, small beads (*i.e.* for glass, $d < 0.4\,\mathrm{mm}$) aggregate either in air or in water which makes the characteristic length be constant and no longer proportional to the bead diameter.

* * *

The authors thank N. Merakchi for his help in preliminary experiments and O. Dauchot for stimulating discussions, and are grateful to Y. C. Zhou and A. B. Yu as well as to Y. Grasselli who have kindly communicated their data. The ACI "Jeunes Chercheurs" no. 2178 and "Prévention des Catastrophes Naturelles" of the French Ministry of Research have supported this work.

REFERENCES

[1] Bagnold R. A., *Proc. R. Soc. London, Ser. A*, **225** (1954) 49.
[2] Van Burkalow A., *Bull. Geol. Soc. Am.*, **56** (1945) 669.
[3] Bocquet L. *et al.*, *Nature*, **396** (1998) 735.
[4] Liu C., Jaeger H. M. and Nagel S. R., *Phys. Rev. A*, **43** (1991) 7092.
[5] Grasselli Y. and Herrmann H. J., *Physica A*, **246** (1997) 301.
[6] Boltenhagen P., *Eur. Phys. J. B*, **12** (1999) 75.
[7] Zhou Y. C., Xu B. H. and Yu A. B., *Phys. Rev. E*, **64** (2001) 021301; Zhou Y. C. *et al.*, *Powder Technol.*, **125** (2002) 45.
[8] Janssen H. A., *Z. Vereins Deutsh Ing.*, **39** (1895) 1045; Duran J., *Sand, Powders and Grains* (Springer, New York) 2000.
[9] Rajchenbach J., *Phys. Rev. Lett.*, **65** (1990) 2221.
[10] Caponeri M. *et al.*, in *Mobile Particulate Systems* (Kluwer, Dordrecht) 1994, p. 331; Dury C. M. *et al.*, *Phys. Rev. E*, **57** (1998) 4491.
[11] Evesque P., *Phys. Rev. A*, **43** (1991) 2720.
[12] The characteristic length of the wall effect increases when significantly increasing the roughness of the lateral walls [6]. This may be explained by a larger friction coefficient μ in eq. (8).
[13] For granular flows on rough inclined planes, Pouliquen (*Phys. Fluids*, **11** (1999) 542) and Daerr and Douady (*Nature*, **399** (1999) 241) show that the angle of repose quickly decreases with an increasing critical material thickness to a constant value with a characteristic length of a few bead diameters. In Couette experiments, velocity profiles in the shear layer of a granular media (Mueth D. M. *et al.*, *Nature*, **406** (2000) 385; Bocquet L. *et al.*, *Phys. Rev. E*, **65** (2001) 011307), as well as the mean velocity of the creep motion of granular surface flow (Komatsu T. S., *Phys. Rev. Lett.*, **86** (2001) 1757) decay exponentially with characteristic lengths of a few bead diameters.
[14] As granular media dilate under shear, the packing fraction of the flowing layer is lower than the one for a static pile. Thus, stress redistribution to the walls may be less efficient with a smaller K value.
[15] Israelachvili J., *Intermolecular and Surface Forces* (Academic Press) 1991.
[16] Albert R. *et al.*, *Phys. Rev. E*, **56** (1997) R6271.